Electrochemistry of $[Mo_2Cp_2(CO)_4\{\mu\text{-}\eta^2\text{:}\eta^3\text{-}HC{\equiv}C{-}C(R1)(R2)\}]^+$ Complexes (R1 = H, R2 = H, Me, Et, Fc; R1 = Me, R2 = Me, Ph). Control of the Reduction Process (Two-Electron *vs* One-Electron) by the Substituents R1 and R2: EHMO Rationalization

Jean-François Capon,[†] René Kergoat,*[,†] Nathalie Le Berre-Cosquer,[†] Stéphane Péron,[‡] Jean-Yves Saillard,*[,§] and Jean Talarmin*[,†]

UMR 6521, Chimie, Electrochimie Moléculaires et Chimie Analytique, Département de Chimie, Université de Bretagne Occidentale, 6 Av V. Le Gorgeu, BP 809, 29285 Brest Cedex, France, Département de Mathématiques, Université de Bretagne Occidentale, 6 Av V. Le Gorgeu, BP 809, 29285 Brest Cedex, France, and UMR 6511, Chimie du Solide et Inorganique Moléculaire, Université de Rennes 1, Campus de Beaulieu, 35042 Rennes Cedex, France

Received April 22, 1997[⊗]

The electrochemical reduction of $[Mo_2Cp_2(CO)_4\{\mu\text{-}\eta^2\text{:}\eta^3\text{-}HC{\equiv}C{-}C(R1)(R2)\}]^+$ complexes has been investigated by cyclic voltammetry, controlled-potential electrolysis, and coulometry. On the cyclic voltammetry time scale, the complexes with R1 = H, R2 = H (**1**$^+$), Me (**2**$^+$), Et (**3**$^+$) undergo an irreversible or a quasi-reversible one-electron reduction whereas the analogues with R1 = H, R2 = Fc (**4**$^+$) and R1 = Me, R2 = Me (**5**$^+$) and Ph (**6**$^+$) reduce in a single-step, reversible or quasi-reversible, two-electron process. Two different chemical reactions are involved in the overall reduction mechanism. The first chemical step is assigned as a structural rearrangement, responsible for slowing down the heterogeneous electron transfer. Extended Hückel MO calculations indicate that in the case of the complexes with R1 = H, R2 = Fc and R1 = Me, R2 = Me or Ph, a small increase in the distance between one metal center and the carbon of the C(R1)(R2) group could trigger the two-electron transfer process. The second chemical reaction leading to the final product(s) of the reduction involves radical species, even when a two-electron transfer is observed by cyclic voltammetry. The final products formed in these processes have been identified either by ^{1}H NMR spectroscopy of the compounds extracted from the catholyte after controlled-potential electrolyses or from a comparison of their characteristic redox potentials with those of authentic samples. The nature of the final product(s), either a dimer or μ-alkyne and μ-enyne complexes, is also dependent on the nature of R1 and R2.

Introduction

Transition metal complexes containing unsaturated hydrocarbons are seen as models of the interactions (bonding mode, reactivity) of these organic molecules at the surface of metal catalysts. The studies related to coordinated hydrocarbon fragments, in particular carbenium ions stabilized *via* coordination to metal centers, have been reviewed recently.[1] One of the objectives of the present study was to determine whether the products of the chemical reduction of the carbenium compounds $[Mo_2Cp_2(CO)_4\{\mu\text{-}\eta^2\text{:}\eta^3\text{-}HC{\equiv}C{-}C(R1)(R2)\}]^+$, *i.e.*, either the dimer, the (μ-alkyne) $[Mo_2Cp_2(CO)_4\{\mu\text{-}HC{\equiv}C{-}C(H)(R1)(R2)\}]$, or the ($\mu$-enyne) $[Mo_2Cp_2(CO)_4\{\mu\text{-}HC{\equiv}C{-}C(R){=}C(R')(R'')\}]$ complexes,[2] resulted from radical processes or from a father−son reaction involving ionic species, Scheme 1. The radical−radical coupling in Scheme 1 (reaction I-2) could account for the formation of the dimer (D), whereas the μ-alkyne (A) or the μ-enyne (E) complexes could arise from the gain (or the loss) of H$^\bullet$ by (from) the radical (reactions 3a or 3b). On the other hand, the formation of these products could result from reactions involving ionic species, as shown in Scheme 1 (reaction II). Indeed, when R1 or R2 has acidic protons, the deprotonation of $[Mo_2Cp_2(CO)_4\{\mu\text{-}\eta^2\text{:}\eta^3\text{-}HC{\equiv}C{-}C(R1)(R2)\}]^+$ by the corresponding anion would give rise to the (μ-enyne) and (μ-alkyne) complexes (Scheme 1, reaction II-3) while nucleophilic attack of the carbenium cation by the corresponding anion could produce the dimer (Scheme 1, reaction II-2)).

During the course of our work, a paper concerning the electrochemistry of $[M_2Cp_2(CO)_4\{\mu\text{-}\eta^2\text{:}\eta^3\text{-}HC{\equiv}C{-}C(R1)(R2)\}]^+$ complexes (M = Mo or W; R1 = H, R2 = H, Me, i-Pr; R1 = R2 = Me) has been published by Strelets *et al.*[3] As some of our conclusions differ from those of these authors, we report herein a full account of our findings. We found that the electrochemical behavior of the carbenium complexes is strongly dependent on the nature of the R1 and R2 substituents and that the complexes can be separated into two groups depending on their reduction mechanism on the cyclic voltammetry time scale; the complexes with R1 = H, R2 = H, Me, or Et undergo a one-electron reduction, whereas the analogues with R1 = H, R2 = Fc and R1 =

[†] UMR 6521, Université de Bretagne Occidentale.
[‡] Département de Mathémathiques, Université de Bretagne Occidentale.
[§] Université de Rennes 1.
[⊗] Abstract published in *Advance ACS Abstracts,* September 15, 1997.

(1) El Amouri, H.; Gruselle, M. *Chem. Rev.* **1996**, *96*, 1077.
(2) Capon, J. F.; Le Berre-Cosquer, N.; Kergoat, R. *J. Organomet. Chem.* **1996**, *508*, 1.
(3) Barinov, I. V.; Kukharenko, S. V.; Strelets, V. V. *Izv. Akad. Nauk., Ser Khim.* **1994**, 417.

S0276-7333(97)00341-5 CCC: $14.00

Scheme 1[a]

I

$C^+ + 1e \longrightarrow C^\bullet$ (1)

$2\,C^\bullet \longrightarrow D$ (2)

$C^\bullet + H^\bullet \longrightarrow A$ (3a)

$C^\bullet - H^\bullet \longrightarrow E$ (3b)

II

$C^+ + 1e \longrightarrow C^\bullet$ (1a)

$C^\bullet + 1e \longrightarrow C^-$ (1b)

or

$C^+ + C^- \longrightarrow D$ (2)

$C^+ + C^- \longrightarrow A + E$ (3)

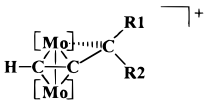

Carbenium complex (C^+)

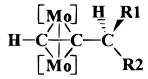

μ-alkyne complex (A)

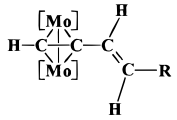

μ-enyne complex (E)

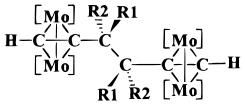

dimer (D)

[a] [Mo] = [Mo(CO)$_2$Cp.

Table 1. Redox Potentials (in V/Fc) of [Mo$_2$Cp$_2$(CO)$_4${μ-η^2:η^3-HC≡C−C(R1)(R2)}]$^+$ Complexes Measured by Cyclic Voltammetry[a]

				products		
R1/R2	solvent	E_p^{red}	n (F/mol)	$E_{1/2}^{ox1}$	E_p^{ox2}	E_p^{red}
H/H	thf	−1.33	0.97	−0.15	0.27	−2.57
	CH_2Cl_2	−1.26		−0.18	0.27	
H/Me	thf	−1.20/−0.80	1.04	−0.08	0.36	−2.57
				−0.16		
	CH_2Cl_2	−1.15/−0.83	0.93	−0.04	0.34	
				−0.15		
H/Et	thf	−1.21/−0.75	1.07	−0.15	0.19	−2.46
	CH_2Cl_2	−1.16/−0.82		−0.17	0.27	
H/Fc	CH_2Cl_2	−0.93 (r)		−0.18	0.05	
Me/Me	thf	−1.05/−0.86		−0.20	0.06	
	CH_2Cl_2	−0.97 (r)	*b*	−0.17	0.22 (qr)	
	MeCN	−0.91 (r)	*b*	−0.17	0.09	
Me/Ph	thf	−0.93 (r)	*b*	−0.14	0.15 (r)	−2.41
	CH_2Cl_2	−0.86 (r)	*b*	−0.15	0.25	
	MeCN	−0.83 (r)	*b*	−0.19	0.15	

[a] Vitreous carbon electrode; scan rate, v = 0.2 V/s; r = reversible, qr = quasi-reversible. [b] See Table 2.

Me, R2 = Me or Ph reduce in an overall two-electron step under the same conditions. Qualitative MO (molecular orbital) calculations undertaken to rationalize these phenomena are discussed.

Results and Discussion

Cyclic Voltammetric Studies. The cyclic voltammetry (cv) of the title complexes is affected by the nature of the solvent, the nature of the electrode (vitreous carbon, Pt), and the surface state of the vitreous carbon disk used throughout this study. The redox potentials of the complexes are listed in Table 1.

R1 = R2 = H (1$^+$). Cyclic voltammetry shows that [Mo$_2$Cp$_2$(CO)$_4${μ-η^2:η^3-HC≡C−CH$_2$}]$^+$, **1**$^+$, undergoes an irreversible reduction, leading to the formation of a product characterized by a reduction at a potential more negative than that of **1**$^+$ and by oxidation processes detected on the reverse scan; the first oxidation of the product is a reversible one-electron step (Figure 1a, thf−Bu_4NPF_6, Table 1). A comparison of the reduction peak current of [Mo$_2$Cp$_2$(CO)$_4${μ-η^2:η^3-HC≡C−CH$_2$}]$^+$ (i_p^{red}) to the current (i_p^{ox}) of the reversible one-electron oxidation of [Mo$_2$Cp$_2$(CO)$_4${μ-HC≡C−CH$_3$}] at the same concentration indicates[4] that the reduction of the carbenium involves a single electron on the cv time scale (i_p^{red}/i_p^{ox} = 0.8 (average)). As the controlled-potential electrolyses (cpe) produce the dimer (see below), the EC process[5] in Scheme 1 (I) could be operative provided reaction I-2 is fast on the cv time scale (scan rate $v \leq$ 1V/s).

Table 2. Coulometric Results of Controlled-Potential Electrolyses of [Mo$_2$Cp$_2$(CO)$_4${μ-η^2:η^3-HC≡C−C(R1)(R2)}]$^+$ Complexes

R1/R2	solvent	n (F/mol)	yield of anion (x %)	theoretical $n = (1 + x/100)$
Me/Me	MeCN	1.09	6.1−7.4	1.06−1.07
Me/Me	MeCN	1.05	7	1.07
Me/Me	CH_2Cl_2	*ca.* 1.0	0	1.0
Me/Ph	MeCN	1.36	54	1.54
Me/Ph	MeCN	1.64	65	1.65
Me/Ph	CH_2Cl_2	1.2	18.9−19.4	1.19
Fc/H	CH_2Cl_2	1.38	43.5	1.44
Fc/H	CH_2Cl_2	1.35	30.5	1.30

R1 = H, R2 = Me, Et. R1 = H, R2 = Me (2$^+$). The cv of **2**$^+$ (Figure 2a) is slightly different from that described above and from the cv's of the analogue with R2 = Et. **2**$^+$ is characterized by an irreversible reduction process, and two products (instead of one for **1**$^+$) showing reversible one-electron oxidations are detected at $E_{1/2}^{ox}$ = −0.15 and −0.04 V (CH_2Cl_2 electrolyte, Table 1). In CH_2Cl_2−Bu_4NPF_6, an additional small peak is observed at −0.83 V on the reverse scan after the reduction has been traversed; the current ratio of this

(4) (a) We assumed that the diffusion coefficient of the carbenium cation is the same as that of the μ-alkyne complex. (b) In CH_2Cl_2−Bu_4NPF_6, the [Mo$_2$Cp$_2$(CO)$_4${μ-HC≡C−R}] complexes undergo at least two reversible or quasi-reversible one-electron oxidation processes, the potentials of which are not strongly affected by the nature of R (R = Me $E_{1/2}^{ox1}$ = −0.18 V, $E_{1/2}^{ox2}$ = 0.27 V; R = Et $E_{1/2}^{ox1}$ = −0.15 V, $E_{1/2}^{ox2}$ = 0.21 V; R = CH_2−Fc $E_{1/2}^{ox1}$ = −0.18 V, $E_{1/2}^{ox2}$ = 0.05 V (a third oxidation is observed at E_p^{ox3} = 0.32 V)). (c) For the electrochemistry of (μ-alkyne) complexes, see: Coates, C.; Connelly, N. G.; Crespo, C. *J. Chem. Soc., Dalton Trans.* **1988**, 2509.

(5) Bard, A. J.; Faulkner, L. R. *Electrochemical Methods. Fundamental and Applications;* Wiley: New York, 1980; Chapter 11, pp 429−485.

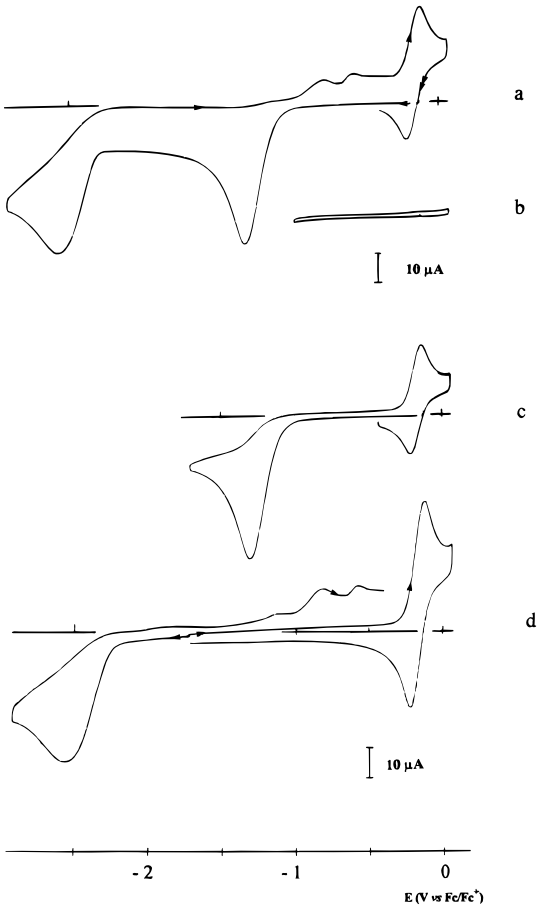

Figure 1. Cyclic voltammetry of $[Mo_2Cp_2(CO)_4\{\mu\text{-}\eta^2\text{:}\eta^3\text{-}HC{\equiv}C{-}CH_2\}]^+$ (**1**$^+$) in thf$-Bu_4NPF_6$: (a, c) before electrolysis and (d) after controlled-potential reduction at −1.5 V (0.98 F/mol cation, Pt cathode). The scan directions in c are the same as in (a). Curves b and c demonstrate that the reversible system at −0.15 V is due to a product generated at the potential of the first reduction (scan rate, 0.2 V/s; vitreous carbon electrode).

peak to the reduction peak of **2**$^+$ increases with increasing scan rate (ratio = 0.08 at 0.2 V/s; 0.30 at 1V/s). As the ratio of the reduction peak current of **2**$^+$ to the peak current of the reversible oxidation of the corresponding μ-alkyne complex, $[Mo_2Cp_2(CO)_4\{\mu\text{-}HC{\equiv}C{-}CH_2{-}CH_3\}]$, at the same concentration is very close to unity ($i_p^{red}/i_p^{ox} = 0.9$), the reduction is assigned as a one-electron step.[4] The peak around −0.8 V is, thus, due to the oxidation of the radical $[Mo_2Cp_2(CO)_4\{\mu\text{-}HC{\equiv}C{-}C(H)(Me)\}]^\bullet$, **2**$^\bullet$, which escaped further reactions leading to the two products on the short time scale of the cv experiment. As a matter of fact, the reduction of $[Mo_2Cp_2(CO)_4\{\mu\text{-}\eta^2\text{:}\eta^3\text{-}HC{\equiv}C{-}C(H)(Me)\}]^+$ is an overall one-electron process on the longer time scale of controlled-potential electrolyses (see below).

R1 = H, R2 = Et (3$^+$). The cv of **3**$^+$ is qualitatively similar in MeCN, thf, and CH_2Cl_2 electrolytes at a vitreous carbon electrode in that an oxidation peak associated with the reduction step is detected on the reverse scan. As shown in Figure 3a, this oxidation partially regenerates the initial complex, making the redox process chemically quasi-reversible on the cv time scale. The question as to whether the reduction is a one-electron or a two-electron step has been addressed, as in the above examples, by comparing the reduction peak current of **3**$^+$ to the current of the reversible

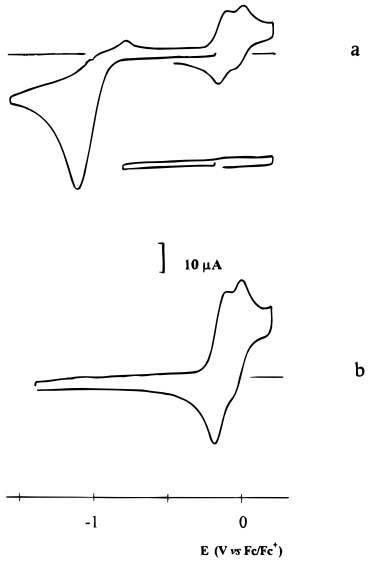

Figure 2. Cyclic voltammetry of $[Mo_2Cp_2(CO)_4\{\mu\text{-}\eta^2\text{:}\eta^3\text{-}HC{\equiv}C{-}C(H)(Me)\}]^+$ (**2**$^+$) in $CH_2Cl_2{-}Bu_4NPF_6$: (a) before electrolysis and (b) after controlled-potential reduction at −1.5 V (0.93 F/mol cation, Pt cathode; scan rate, 0.2 V/s; vitreous carbon electrode).

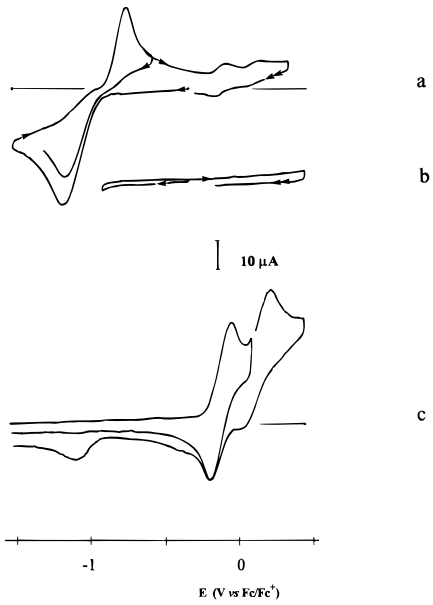

Figure 3. Cyclic voltammetry of $[Mo_2Cp_2(CO)_4\{\mu\text{-}\eta^2\text{:}\eta^3\text{-}HC{\equiv}C{-}C(H)(Et)\}]^+$ (**3**$^+$) in thf$-Bu_4NPF_6$: (a) before electrolysis and (c) after controlled-potential reduction at −1.5 V (0.84 F/mol cation, Pt cathode; scan rate, 0.2 V/s; vitreous carbon electrode).

oxidation of $[Mo_2Cp_2(CO)_4\{\mu\text{-}HC{\equiv}C{-}CH_2{-}CH_3\}]$ at the same concentration.[4a] The peak current ratio measured in thf$-Bu_4NPF_6$ and in $CH_2Cl_2{-}Bu_4NPF_6$ is $i_p^{red}/i_p^{ox} \approx 1.1$, which means that the reduction of the cation is a one-electron process, and therefore, the peak detected around −0.7 or −0.8 V on the reverse scan is due to the oxidation of the radical $[Mo_2Cp_2(CO)_4\{\mu\text{-}HC{\equiv}C{-}C(H)(Et)\}]^\bullet$, **3**$^\bullet$. The reduction is a diffusion-controlled process with linear plots of $i_p/v^{1/2} = f(v)$ (0.01 V/s $\le v \le$ 1 V/s) and $i_t = f(t^{-1/2})$ (0.5 s $\le t \le$ 10 s) ($CH_2Cl_2{-}Bu_4NPF_6$). The scan-rate dependence of the current ratio of the reduction peak (i_p^c) to the associated oxidation peak (i_p^a) ($(i_p^a/i_p^c) = 0.26$ for $v = 0.02$ V/s; *ca.* 0.8 for 0.1 V/s $\le v \le$ 1 V/s, CH_2Cl_2 electrolyte) indicates the occurrence of an EC process. Similar results were obtained in MeCN−

Bu_4NPF_6, where (i_p^a/i_p^c) increases from 0.32 for $v = 0.02$ V/s to *ca.* 0.7 for 0.1 V/s $\leq v \leq 1$ V/s. In agreement with this result, redox couples due to the final products of the EC reduction are observed around 0 V (Figure 3a), but these are much smaller for $\mathbf{3}^+$ than for $\mathbf{1}^+$ or $\mathbf{2}^+$.

The cathodic-to-anodic peak separation of the reduction process, ΔE_p, increases from 265 mV at $v = 0.02$ V/s to 395 mV at 1 V/s in a CH_2Cl_2 electrolyte (ΔE_p = 248 and 320 mV, respectively, in MeCN−Bu_4NPF_6). Cyclic voltammograms with large ΔE_p values can be found when a chemical reaction (for example a structural rearrangement) is coupled after (or concomitant with) the electron-transfer step,[6,7] since the energy required to rearrange the molecule contributes to the activation barrier to the heterogeneous electron transfer; this results in slow electron-transfer kinetics. In the present case, however, the slow kinetics of the electron transfer is not only due to a structural modification; other factors (solvation, interfacial phenomena) must contribute to the activation barrier, as shown by the dependence of the cyclic voltammograms on the solvent and the nature of the electrode.

It often proves difficult to determine whether the observed phenomena belong to the quasi-reversible case or to the four-component scheme described by Geiger[6] and Evans.[7] In the present case, attempts to detect other species possibly involved in the redox process, that is attempts to make the reduction and/or the oxidation reversible, were unsuccessful. Lowering the temperature (or increasing the scan rate) only resulted in a wider separation between the reduction and the associated oxidation peak. We, therefore, favor the first possibility, a quasi-reversible process with slow heterogeneous electron transfer due to a chemical reaction coupled to the electron-transfer step.

The results concerning the reduction of the $[Mo_2Cp_2(CO)_4\{\mu\text{-}\eta^2\text{:}\eta^3\text{-}HC{\equiv}C{-}C(H)(R)\}]^+$ complexes with R = H or Me are quite different from those reported recently.[3] We found that both of these complexes undergo a one-electron reduction, whereas Strelets *et al.*[3] reported reversible two-electron reductions (ECE) on the cv time scale (Hg electrode) in a thf−Bu_4NBF_4 electrolyte. Furthermore, under our experimental conditions, the process is chemically irreversible since no oxidation peak (other than those of the final products) or a very small one (for R = Me) was detected on the reverse scan. The reduction of $[Mo_2Cp_2(CO)_4\{\mu\text{-}\eta^2\text{:}\eta^3\text{-}HC{\equiv}C{-}C(H)(Et)\}]^+$, $\mathbf{3}^+$, is a one-electron, chemically quasi-reversible process; the cv obtained at a vitreous carbon electrode is qualitatively similar to that of $[Mo_2Cp_2(CO)_4\{\mu\text{-}\eta^2\text{:}\eta^3\text{-}HC{\equiv}C{-}C(H)(i\text{-}Pr)\}]^+$ recorded at a Pt electrode.[3] The nature of the electrode can be responsible for differences in the charge-transfer kinetics of a redox couple,[6] as shown in the case of $[Mo_2Cp_2(CO)_4\{\mu\text{-}\eta^2\text{:}\eta^3\text{-}HC{\equiv}C{-}C(H)(i\text{-}Pr)\}]^+$ (Hg *vs* Pt electrode) where this was assigned to H-atom abstraction from the radical complexes by the Pt electrode.[3] Enhanced reversibility on mercury has also been attributed to the stabilization of one partner of the redox couple by a covalent interaction with the electrode.[8] In the case of the $[Mo_2Cp_2(CO)_4\{\mu\text{-}\eta^2\text{:}\eta^3\text{-}HC{\equiv}C{-}C(H)(R)\}]^+$ complexes, such an interaction could stabilize the radical and "protect" it from the reactions which lead to the final products observed on the cv time scale (and formed by cpe) under our experimental conditions (cv, vitreous carbon electrode; cpe, Pt electrode). Other authors have attributed the slow electron-transfer kinetics observed on Pt electrodes to the formation of an insulating film[9] or to the contamination of the electrode.[10]

R1 = H, R2 = Fc ($\mathbf{4}^+$). The reduction of $\mathbf{4}^+$ has been investigated only in CH_2Cl_2−Bu_4NPF_6, where a quasi-reversible reduction and a reversible oxidation are observed. In thf−Bu_4NPF_6 and MeCN−Bu_4NPF_6, the cv showed a very broad reduction peak, and the electrochemistry was not investigated further in these electrolytes. In $\mathbf{4}^+$, the carbenium ion is stabilized by two organometallic moieties, *i.e.*, the dimolybdenum fragment and the ferrocenyl group, the latter being responsible for the one-electron oxidation at $E_{1/2}^{ox} = 0.15$ V (Table 1) which was not observed in the other carbenium compounds described above. The peak current of the reversible one-electron oxidation (i_p^{ox}) was used as an internal standard to calibrate the current of the quasi-reversible reduction step (i_p^{red}) at $E_{1/2}^{red} = -0.93$ V (Table 1). The mean value of the i_p^{red}/i_p^{ox} ratio measured at different scan rates ($i_p^{red}/i_p^{ox} = 2.1$) demonstrates that the reduction of $\mathbf{4}^+$ is a two-electron process on the cv time scale. The anodic-to-cathodic peak separation for the reduction process, $\Delta E_p = 56$ mV at $v = 0.01$ V/s, increases with increasing scan rate (ΔE_p = 140 mV at $v = 1$ V/s), and the potential of the reduction peak shifts cathodically with increasing v (slope −25 mV per 10-fold increase in v), which shows that the electron-transfer steps are not fully reversible. It has been shown that for "single-step" two-electron-transfer processes with the standard potential of the second electron-transfer less negative (for a reduction) than, or equal to, that for the first one ($|E°_1| \geq |E°_2|$), the shape of the cv curves (peak separation, peak currents) is strongly dependent on the magnitudes of $\Delta E° = E°_2 - E°_1$, $k°_i$ (the standard heterogeneous rate constants of these steps), and the k_1/k_2 ratio.[11−13] For reversible processes with fast heterogeneous electron transfers, the theoretical peak separation is $\Delta E_p = 29.5$ mV when $|E°_1| > |E°_2|$ and $\Delta E_p = 42$ mV for $|E°_1| = |E°_2|$.[11,14] Therefore, the reduction of $[Mo_2Cp_2(CO)_4\{\mu\text{-}\eta^2\text{:}\eta^3\text{-}HC{\equiv}C{-}C(H)(Fc)\}]^+$ is assigned as a quasi-reversible single-step two-electron transfer with $|E°_1| \geq |E°_2|$.

R1 = Me, R2 = Me ($\mathbf{5}^+$) or Ph ($\mathbf{6}^+$). The reduction of $\mathbf{6}^+$ is quasi-reversible on the cv time scale at room temperature in thf−, CH_2Cl_2−, or MeCN−electrolyte (Figure 4a, Table 1). The anodic-to-cathodic peak separation, ΔE_p, which is 90 mV at a scan rate of 0.2 V/s in thf−Bu_4NPF_6 decreases to 60 mV in CH_2Cl_2 (v = 0.02V/s) and to 51 and 43 mV in MeCN−Bu_4NPF_6 for v = 0.02 and 0.01 V/s, respectively. These values of ΔE_p indicate that the reduction involves the transfer of two electrons, with $|E°_1| \geq |E°_2|$. The negative shift of E_p^{red} with increasing scan rate (slope *ca.* −33 mV per 10-fold

(6) Geiger, W. E. *Prog. Inorg. Chem.* **1985**, *33*, 275.
(7) Evans, D. H.; O'Connell, K. M. In *Electroanalytical Chemistry*; Bard,A. J., Ed.; M. Dekker: New York, 1986; Vol. 14, p 113.
(8) Blanch, S. W.; Bond, A. M.; Colton, R. *Inorg. Chem.* **1981**, *20*, 755.
(9) Amatore, C.; Savéant, J. M.; Tessier, D. *J. Electroanal. Chem.* **1983**, *146*, 37; *Ibid.* **1983**, *147*, 39.
(10) Bowyer, W. J.; Geiger, W. E. *J. Electroanal. Chem.* **1988**, *239*, 253.
(11) Polcyn, D. S.; Shain, I. *Anal. Chem.* **1966**, *38*, 370.
(12) Hinkelmann, K.; Heinze, J. *Ber. Bunsen-Ges. Phys. Chem.* **1987**, *91*, 243.
(13) Ryan, M. D. *J. Electrochem. Soc.* **1978**, *125*, 547.
(14) Heinze, J. *Angew. Chem., Int. Ed. Engl.* **1984**, *23*, 831.

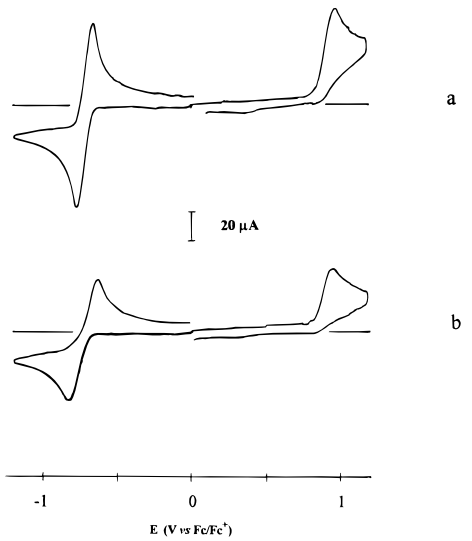

Figure 4. Cyclic voltammetry of a solution of $[Mo_2Cp_2(CO)_4\{\mu\text{-}\eta^2\text{:}\eta^3\text{-}HC{\equiv}C{-}C(Me)(Ph)\}]^+$ (**6**$^+$) (*ca.* 1 mM) in $CH_2Cl_2{-}Bu_4NPF_6$: (a) at room temperature and (b) at −40 °C (scan rate, 0.2 V/s; vitreous carbon electrode).

increase in v) and the fact that lowering the temperature leads to a wider separation of the cathodic and anodic peaks (Figure 4b, T = *ca.* −40 °C) confirm that the electron-transfer steps are not fully reversible.

The analogue with R2 = Me, **5**$^+$, shows a wider separation of the peaks (ΔE_p = 65 mV in MeCN−Bu_4NPF_6 at a scan rate of v = 0.01 V/s) and a smaller peak current ratio in thf−Bu_4NPF_6 [$(i_p^a/i_p^c)_{red} < 1$] than in MeCN− or $CH_2Cl_2{-}Bu_4NPF_6$. Comparison of the reduction peak current ($i_p^{c}{}_{red}$) to the current (i_p^{ox}) of the reversible oxidation of $[Mo_2Cp_2(CO)_4\{\mu\text{-}HC{\equiv}C{-}CH_2{-}CH_3\}]$ at the same concentration indicates[4a] that two electrons are involved in the reduction step ($i_p^{c}{}_{red}/i_p^{ox}$ = 1.74, v = 0.2 V/s, $CH_2Cl_2{-}Bu_4NPF_6$). The fact that the electron transfers are not fully reversible is illustrated by the increase of ΔE_p from 70 mV at v = 0.01 V/s to 210 mV at v = 1 V/s ($CH_2Cl_2{-}Bu_4NPF_6$) and by the negative shift of the reduction peak with increasing scan rate in this electrolyte: the slope of the line $E_p^{c}{}_{red}$ = f(log v) is about −38 mV.

The redox potentials listed in Table 1 show a dependence on the nature of the R1 and R2 substituents, which suggests that the LUMO or some of the lowest vacant orbitals of the complexes receive a contribution from the carbenium ligand. The complex with R1 = R2 = H is more difficult to reduce than the singly- or doubly-substituted analogues. Substitution of a methyl group for a hydrogen atom leads to a positive shift by 110 mV of the reduction potential; a second substitution results in a further positive shift by *ca.* 180 mV. It can be noted that the compounds which undergo a two-electron-transfer process on the cv time scale are easier to reduce than those which undergo a one-electron reduction.

Controlled-Potential Electrolyses. R1= H, R2 = H, Me. As shown by the ^{1}H NMR spectroscopy of the compounds extracted from the catholytes, the controlled-potential electrolyses of **1**$^+$ and **2**$^+$ at a potential 100 mV more negative than E_p^{red} lead to the quantitative formation of the dimers after consumption of 1 F/mol of starting material (Figures 1d and 2b, Table 1). In the case of the methyl-substituted carbenium complex, the occurrence of two peaks on the cv time scale as well as after cpe arises from the formation of the previously characterized[15] stereoisomers of the dimer.

R1 = H, R2 = Et (3$^+$). The reduction of **3**$^+$ is an overall one-electron process in thf and CH_2Cl_2 electrolytes (Table 1). In both solvents, products showing one reversible and one irreversible oxidation are formed (Figure 3c, Table 1). ^{1}H NMR analysis of the products obtained by reduction in thf−Bu_4NPF_6 (*ca.* 1 F/mol of **3**$^+$) showed that $[Mo_2Cp_2(CO)_4\{\mu\text{-}HC{\equiv}C{-}CH_2\text{-}Et\}]$[4c] and $[Mo_2Cp_2(CO)_4\{\mu\text{-}HC{\equiv}C{-}C(H){=}C(H)(Me)\}]$ were present in an approximately equimolar ratio (*ca.* 60/40) (Scheme 2), although only one reversible (one-electron) and one irreversible oxidation were observed in the cv of the catholyte.

R1= H, R2 = Fc; R1 = Me, R2 = Me, Ph. Controlled-potential electrolysis of the complexes with R1 = H, R2 = Fc (**4**$^+$) and R1 = Me, R2 = Ph (**6**$^+$) carried out in MeCN− or $CH_2Cl_2{-}Bu_4NPF_6$ at a potential 100 mV more negative than E_p^{red} are similar in that some $[Mo_2Cp_2(CO)_4\{\mu\text{-}HC{\equiv}C{-}C(R1)(R2)\}]^-$ is produced along with neutral complexes in variable amounts (Table 2). In the case of the dimethyl analogue **5**$^+$, cpe in MeCN produces a small amount of the anion (5−7%, Figure 5a, bottom curve) whereas no anion is detected after electrolysis in CH_2Cl_2 (Figure 5b, bottom curve) (Table 2). The latter situation is quite analogous to the case described above for the complex with R1 = H, R2 = Et since ^{1}H NMR analysis of the products resulting from the reduction of $[Mo_2Cp_2(CO)_4\{\mu\text{-}\eta^2\text{:}\eta^3\text{-}HC{\equiv}C{-}C(Me)_2\}]^+$, **5**$^+$, in CH_2Cl_2 revealed the formation of the μ-alkyne $[Mo_2Cp_2(CO)_4\{\mu\text{-}HC{\equiv}C{-}CH(Me)_2\}]$ and μ-enyne $[Mo_2Cp_2(CO)_4\{\mu\text{-}HC{\equiv}C{-}C(Me){=}CH_2\}]$ complexes in equivalent amounts.

In the other situations, the yield of the anion was calculated from the currents of the reversible redox couple of the complex measured before and after electrolysis. The yield of the anion and the number of electrons consumed in the cpe are consistent only with the mechanism presented in Scheme 3, which shows that the radical species is the precursor of the final neutral product(s) P. In the case of the cation with R1 = H, R2 = Fc, P is assigned as $[Mo_2Cp_2(CO)_4\{\mu\text{-}HC{\equiv}C{-}CH_2\text{-}Fc\}]$ from a comparison with the potentials of an authentic sample of this complex.[4b]

The mechanism in scheme 3 has been verified in the following ways. (i) controlled-potential oxidation of the $[Mo_2Cp_2(CO)_4\{\mu\text{-}HC{\equiv}C{-}C(Me)(Ph)\}]^-$ anion produced by cpe of the corresponding cation regenerates some starting material (*ca.* 30% of the initial concentration), while the current for the oxidation processes around −0.15 and 0.15 V (MeCN) due to the neutral co-product P has increased. The formation of the co-product during *both* the reduction of the parent cation and the oxidation of the corresponding anion strongly suggests that it results from a chemical reaction of the radical, thermodynamically unstable intermediate of the two-electron process. (ii) A solution of the electrogenerated anion $[Mo_2Cp_2(CO)_4\{\mu\text{-}HC{\equiv}C{-}C(Me)(Ph)\}]^-$ (Figure 6b) was stirred under argon for 1 h,[16] during which time its reversible oxidation decreased by less than 30% whereas

(15) Le Berre-Cosquer, N.; Kergoat, R.; L'Haridon, P. *Organometallics* **1992**, *11*, 721.

(16) This is more than the duration of the controlled-potential oxidation of the same amount of $[Mo_2Cp_2(CO)_4\{\mu\text{-}HC{\equiv}C{-}C(Me)(Ph)\}]^-$ which requires *ca.* 40 min.

Scheme 2

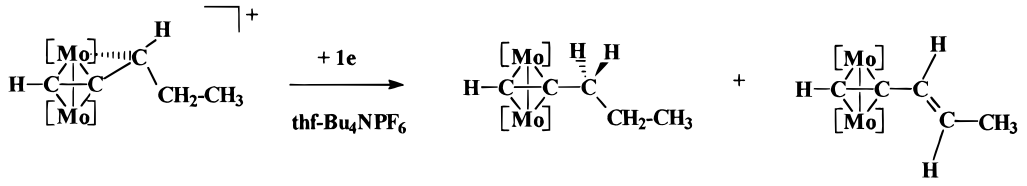

the reversible oxidation of the neutral co-product increases by approximately 20%. A new, minor redox process is also observed around −0.67 V (Figure 6c). The anion was then oxidized (duration < 40 min), and the cv of the resulting solution is shown in Figure 6d: it can be seen that the redox couple associated with $[Mo_2Cp_2(CO)_4\{\mu\text{-HC}\equiv\text{C}-\text{C(Me)(Ph)}\}]^{-/+}$ has decreased by 65% whereas the oxidation current of the neutral product increased by *ca.* 60%. This demonstrates that the final product arises essentially from a reaction involving the radical, while the reaction of the anion appears slower and may also produce the unknown species with the redox system at −0.67 V.

Coupled Chemical Reactions. As mentioned above, the large peak separation (ΔE_p) is partly due to solvation and interfacial phenomena. However, since the reduction of all the complexes was studied under the same experimental conditions, particularly using the same vitreous carbon disk electrode, it is possible to draw qualitative conclusions from the above results. These results demonstrate that two different chemical reactions are involved in the reduction of the carbenium complexes: the first one is responsible for slow electron-transfer kinetics and ΔE_p values larger than those for Nernstian redox couples. For complexes $\mathbf{1}^+-\mathbf{3}^+$, the radical arising from this process is quantitatively converted into products on the time scale of controlled-potential electrolyses by the second chemical step, whereas some anion $\mathbf{4}^- - \mathbf{6}^-$ is observed after completion of the electrolyses of the corresponding cations, depending on the solvent used. As the radical cannot be isolated and the anion $\mathbf{4}^- - \mathbf{6}^-$ could not be separated from the supporting electrolyte, the nature of the first chemical step cannot be determined precisely. We assign it as a structural rearrangement since a reaction involving ligand loss seems unlikely in the compounds under study. Although both chemical reactions are detected on the cv time scale for the complexes with R1 = H, R2 = Me or Et, the first one is coupled to (or concomitant with) the electron transfer whereas the second involves the rearranged radical arising from the one-electron reduction. When R1 = R2 = H, the rate of the second reaction is such that the primary product of the electron transfer is not detected under our experimental conditions ($v \leq 1$ V/s). The chemical reactions will be analyzed separately below.

Structural Rearrangement. The $[Mo_2Cp_2(CO)_4\{\mu\text{-}\eta^2\text{:}\eta^3\text{-HC}\equiv\text{C}-\text{C(R1)(R2)}\}]^+$ complexes can be classified into two different groups depending on whether their reduction is a one-electron or a two-electron process on the cv time scale. Thus, the derivatives with R1 = H, R2 = H, Me, or Et ($\mathbf{1}^+-\mathbf{3}^+$) undergo a one-electron reduction on the cv time scale, whereas the reduction of the analogues with R1 = H, R2 = Fc and R1 = Me, R2 = Me or Ph ($\mathbf{4}^+-\mathbf{6}^+$) is a quasi-reversible, single-step two-electron transfer under the same conditions. This could arise from a different composition of the lowest unoccupied MO's for the two groups. The fact that the complexes of the second group undergo a single step two-electron reduction indicates that the addition of the first electron causes a modification such as stabilization of the semioccupied orbital (SOMO) results; this stabilization, in turn, favors the transfer of a second electron at the same potential as the first. This type of situation has already been found in dimolybdenum thiolate-bridged complexes where the LUMO is a Mo−Mo antibonding orbital.[17] For the complexes of the first group, the addition of the first electron also causes substantial reorganization within the radical, as shown by the large peak separation. In this case though, the structural change does not favor the transfer of a second electron.

The main difference between the differently substituted carbenium complexes which have been characterized crystallographically so far lies in the Mo1−C5 distance (Scheme 4). The X-ray crystal structure of various $[Mo_2Cp_2(CO)_4\{\mu\text{-}\eta^2\text{:}\eta^3\text{-HC}\equiv\text{C}-\text{C(R1)(R2)}\}]^+$ cations have shown a Mo1···C5 interaction, the strength of which (estimated from the distance between these atoms)[18,19] decreases with the increasing size of the R1 and R2 substituents. Thus, the Mo1···C5 distance is longer (and the interaction is weaker) in $[Mo_2Cp_2(CO)_4\{\mu\text{-}\eta^2\text{:}\eta^3\text{-HC}\equiv\text{C}-\text{C(Me)}_2\}]^+$ (d(Mo1···C5) = 2.75(1) Å[20]) than in the analogues with R1 = H, R2 = Me (d(Mo1···C5) = 2.613 Å[15]) and R1 = R2 = H (d(Mo1···C5) = 2.439(6) Å[20]). This distance should be similar in $[Mo_2Cp_2(CO)_4\{\mu\text{-HC}\equiv\text{C}-\text{C(H)(Et)}\}]^+$ and $[Mo_2Cp_2(CO)_4\{\mu\text{-}\eta^2\text{:}\eta^3\text{-HC}\equiv\text{C}-\text{C(Me)(Ph)}\}]^+$ to those observed in $[Mo_2Cp_2(CO)_4\{\mu\text{-}\eta^2\text{:}\eta^3\text{-HC}\equiv\text{C}-\text{C(H)(Me)}\}]^+$ and $[Mo_2Cp_2(CO)_4\{\mu\text{-}\eta^2\text{:}\eta^3\text{-HC}\equiv\text{C}-\text{C(Me)}_2\}]^+$, respectively. On the other hand, substitution of one $\{MoCp(CO)_2\}$ fragment by the isoelectronic $\{Co(CO)_3\}$ group does not substantially affect the Mo1···C5 distance, since for $[Mo_2Cp_2(CO)_4\{\mu\text{-}\eta^2\text{:}\eta^3\text{-HC}\equiv\text{C}-\text{C(H)(Me)}\}]^+$ [15] and $[MoCp(CO)_2Co(CO)_3\{\mu\text{-}\eta^2\text{:}\eta^3\text{-HC}\equiv\text{C}-\text{C(H)(Me)}\}]^+$ [21], d(Mo1···C5) is 2.613 and 2.64 Å, respectively. Similarly, d(Mo1···C5)

(17) For "single step" two-electron transfer, see: Collman, J. P.; Rothrock, R. K.; Finke, R. G.; Moore, E. J.; Rose-Munch, F. *Inorg. Chem.* **1982**, *21*, 146. van der Linden, J. G. M.; Paulissen, M. L. H.; Schmits, J. E. J. *J. Am. Chem. Soc.* **1983**, *105*, 1903. Courtot-Coupez, J.; Guéguen, M.; Guerchais, J. E.; Pétillon, F. Y.; Talarmin, J. *J. Organomet. Chem.* **1986**, *312*, 81. Smith, D. A.; Zhuang, B.; Newton, W. E.; McDonald, J. W.; Schultz, F. A. *Inorg. Chem.* **1987**, *26*, 2524. Guéguen, M.; Pétillon, F. Y.; Talarmin, J. *Organometallics* **1989**, *8*, 148. Fernandes, J. B.; Zhang, L. Q.; Schultz, F. A. *J. Electroanal. Chem.* **1991**, *297*, 145. Evans, D. H.; Hu, K. *J. Chem. Soc., Faraday Trans.* **1996**, *92*, 3983. Hu, K.; Evans, D. H. *J. Phys. Chem.* **1996**, *100*, 3030 and references cited therein.

(18) Cordier, C.; Gruselle, M.; Vaissermann, J.; Troitskaya, L. L.; Bakhmutov, V. I.; Sokolov, V. I.; Jaouen, G. *Organometallics* **1992**, *11*, 3825.

(19) McClain, M. D.; Hay, M. S.; Curtis, M. D.; Kampf, J. W. *Organometallics* **1994**, *13*, 4377.

(20) Barinov, I. V.; Reutov, O. A.; Polyakov, A. V.; Yanovsky, A. I.; Struchkov, Y. T.; Sokolov, V. I. *J. Organomet. Chem.* **1991**, *418*, C24.

(21) Gruselle, M.; Kondratenko, M. A.; El Amouri, H.; Vaissermann, J. *Organometallics* **1995**, *14*, 5242.

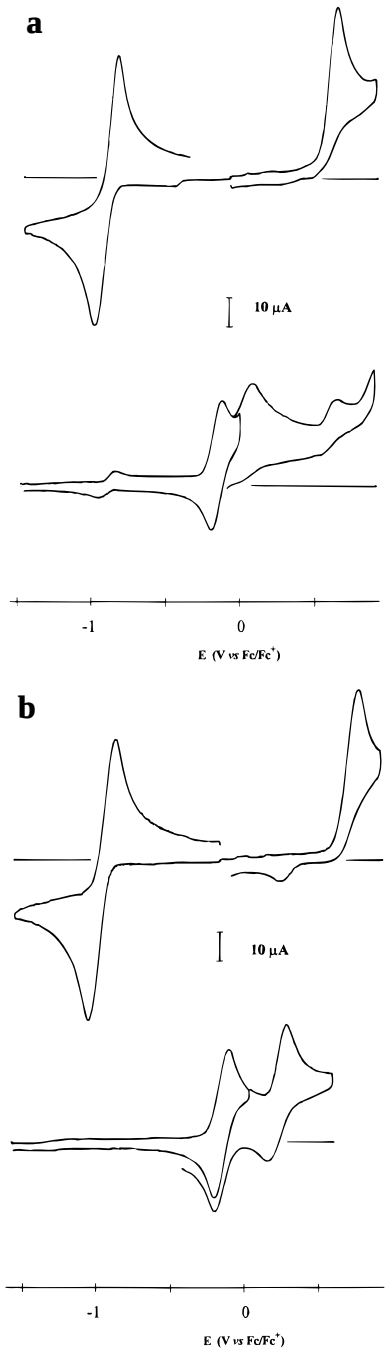

Figure 5. (a) Cyclic voltammetry of $[Mo_2Cp_2(CO)_4\{\mu\text{-}\eta^2\text{:}\eta^3\text{-}HC{\equiv}C{-}C(Me)_2\}]^+$ ($\mathbf{5}^+$) (*ca.* 1 mM) in $MeCN{-}Bu_4NPF_6$ before (top) and after (bottom) controlled-potential reduction at −0.97 V (1.05 F/mol cation, Pt cathode), showing the presence of *ca.* 7% $[Mo_2Cp_2(CO)_4\{\mu\text{-}HC{\equiv}C{-}C(Me)_2\}]^-$ in the catholyte. (b) Cyclic voltammetry of $[Mo_2Cp_2(CO)_4\{\mu\text{-}\eta^2\text{:}\eta^3\text{-}HC{\equiv}C{-}C(Me)_2\}]^+$ ($\mathbf{5}^+$) (1.4 mM) in $CH_2Cl_2{-}Bu_4NPF_6$ before (top) and after (bottom) controlled-potential reduction at −1.18 V (0.85 F/mol cation, Pt cathode), showing that no $[Mo_2Cp_2(CO)_4\{\mu\text{-}HC{\equiv}C{-}C(Me)_2\}]^-$ is present. (Scan rate, 0.2 V/s; vitreous carbon electrode.)

in $[Mo_2Cp_2(CO)_4\{\mu\text{-}\eta^2\text{:}\eta^3\text{-}HC{\equiv}C{-}C(H)(Fc)\}]^+$ should be similar to that found in $[MoCp(CO)_2Co(CO)_3\{\mu\text{-}\eta^2\text{:}\eta^3\text{-}CH_3C{\equiv}C{-}C(H)(Fc)\}]^+$ (2.726 Å[22]).

Therefore, it appears that among the complexes structurally characterized, those which have the largest

(22) Kondratenko, M. A.; Rager, M.-N.; Vaissermann, J.; Gruselle, M. *Organometallics* **1995**, *14*, 3802.

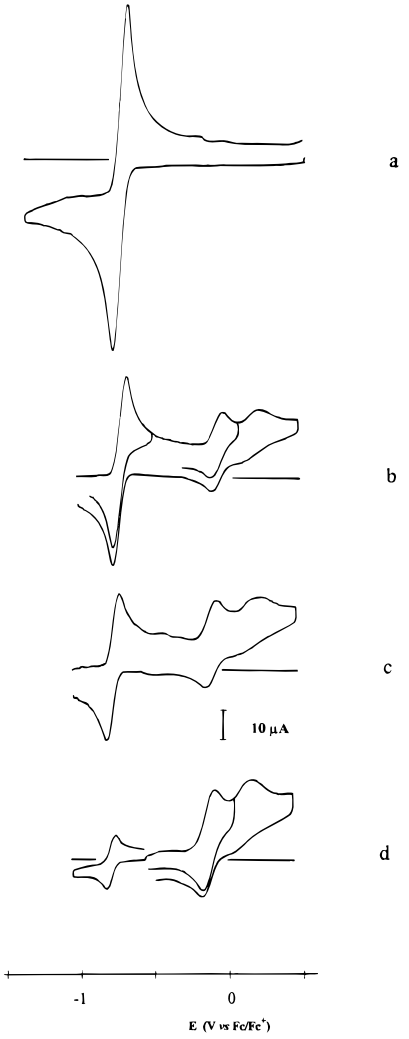

Figure 6. Cyclic voltammetry of (a) $[Mo_2Cp_2(CO)_4\{\mu\text{-}\eta^2\text{:}\eta^3\text{-}HC{\equiv}C{-}C(Me)(Ph)\}]^+$ ($\mathbf{6}^+$) (*ca.* 1 mM) in $MeCN{-}Bu_4NPF_6$, (b) the same solution as in (a) after reduction at −0.95 V (1.4 F/mol cation, Pt cathode), (c) the same solution as in b after 1 h of stirring under Ar, (d) the same solution as in c after controlled-potential oxidation at −0.6 V (0.5 F/mol initial cation, Pt anode). (Scan rate, 0.2 V/s; vitreous carbon electrode).

Scheme 3

$$C^+ + 1\,e \longrightarrow C^\bullet$$

$$x\,C^\bullet + x\,e \longrightarrow x\,C^-$$

$$(1-x)\,C^\bullet \pm y\,H^\bullet \longrightarrow P$$

$$C^+ + (1+x)\,e \pm y\,H^\bullet \longrightarrow x\,C^- + P$$

Mo1···C5 separations in the solid state are also those which undergo a single-step two-electron reduction, whereas shorter Mo1···C5 distances could be associated with one-electron-reduction processes. In order to verify whether the variation in this parameter could be responsible for the different electrochemical behavior of the complexes, we have undertaken molecular orbital calculations.

Theoretical Considerations. The behavior upon reduction of a given molecule is generally related to the composition and energy of its LUMO or of some of it lowest unoccupied MOs. Therefore, the separation of

Scheme 4

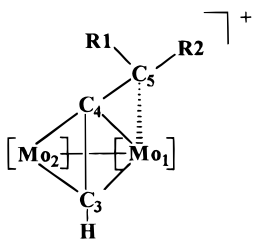

$[Mo_2]-[Mo_1] = Cp(CO)_2Mo-Mo(CO)_2Cp$

the $[Mo_2Cp_2(CO)_4\{\mu\text{-}\eta^2\text{:}\eta^3\text{-}HC{\equiv}C{-}C(R1)(R2)\}]^+$ complexes into two groups depending on their electrochemistry should be related to some differences in their lowest vacant levels. This is why we have carried out extended Hückel (EH) calculations on one model as an example of each group, namely $[Mo_2Cp_2(CO)_4\{\mu\text{-}\eta^2\text{:}\eta^3\text{-}HC{\equiv}C{-}CH_2\}]^+$ and $[Mo_2Cp_2(CO)_4\{\mu\text{-}\eta^2\text{:}\eta^3\text{-}HC{\equiv}C{-}CMe_2\}]^+$. The geometries used in the calculations were taken from the published experimental structural data of the cations considered[15,20] (see Experimental Section). The $[Mo_2Cp_2(CO)_4\{\mu\text{-}\eta^2\text{:}\eta^3\text{-}HC{\equiv}C{-}CMe_2\}]^+$ complex[20] was modeled by changing its Me groups into H atoms. This model will be named $[Mo_2Cp_2(CO)_4\{\mu\text{-}\eta^2\text{:}\eta^3\text{-}HC{\equiv}C{-}CR_2\}]^+$ in the following discussion. A detailed analysis of the interaction of the $\{Mo_2Cp_2(CO)_4\}$ moiety with the organic cation $\{HC{\equiv}C{-}C(R1)(R2)\}^+$ has been reported for R1 = R2 = H[19,23] and for related silylium derivatives.[24] In this paper, we analyze the differences in the localization and energy of the lowest unoccupied orbitals for differently substituted carbenium complexes.

The lowest vacant MOs of a molecule are generally antibonding levels associated to its weakest bonds. In a $[Mo_2Cp_2(CO)_4\{\mu\text{-}\eta^2\text{:}\eta^3\text{-}HC{\equiv}C{-}C(R1)(R2)\}]^+$ complex, the weakest bonding interactions are expected to be π-type C−O bonds, as well as the σ-type Mo1−Mo2 and Mo1−C5 single bonds (Scheme 4). As a matter of fact, the lowest levels of $[Mo_2Cp_2(CO)_4\{\mu\text{-}\eta^2\text{:}\eta^3\text{-}HC{\equiv}C{-}CH_2\}]^+$ and $[Mo_2Cp_2(CO)_4\{\mu\text{-}\eta^2\text{:}\eta^3\text{-}HC{\equiv}C{-}CR_2\}]^+$ exhibit Mo1−Mo2 and/or Mo1−C5 antibonding character, together with significant π*(CO) participation. The latter being more or less constant in all of the calculated models, we will focus the discussion on the variation of the localization of the empty levels on the Mo1−Mo2 and Mo1−C5 bonds.

The MO-level ordering of $[Mo_2Cp_2(CO)_4\{\mu\text{-}\eta^2\text{:}\eta^3\text{-}HC{\equiv}C{-}CH_2\}]^+$ is shown in Figure 7, together with a plot giving the orbital to orbital Mo1−Mo2 and Mo1−C5 overlap populations. One can see that the LUMO is significantly Mo1−Mo2 antibonding (corresponding overlap population = −0.062). The occupation of this LUMO by two electrons would fully cancel the Mo1−Mo2 interaction (resulting total overlap population = −0.001). On the other hand, the LUMO and its next vacant level have no significant Mo1−C5 character. The Mo1−C5 bond is rather short in this complex (2.44 Å), and consequently, the orbitals bearing significant Mo1−C5 character lie at higher energy. This is not the case for $[Mo_2Cp_2(CO)_4\{\mu\text{-}\eta^2\text{:}\eta^3\text{-}HC{\equiv}C{-}CR_2\}]^+$, for which the Mo1−C5 separation is longer (2.75 Å). The plot of its Mo1−C5 overlap population (Figure 8) indicates a large antibonding character in the second lowest unoccupied MO (corresponding value = −0.074). When summed over the four lowest unoccupied levels of $[Mo_2Cp_2(CO)_4\{\mu\text{-}\eta^2\text{:}\eta^3\text{-}HC{\equiv}C{-}CR_2\}]^+$, the Mo1−C5 overlap population is −0.140. In the case of $[Mo_2Cp_2(CO)_4\{\mu\text{-}\eta^2\text{:}\eta^3\text{-}HC{\equiv}C{-}CH_2\}]^+$, it is only −0.037. Conversely, the LUMO of $[Mo_2Cp_2(CO)_4\{\mu\text{-}\eta^2\text{:}\eta^3\text{-}HC{\equiv}C{-}CR_2\}]^+$ has about half the Mo1−Mo2 antibonding character of the LUMO of $[Mo_2Cp_2(CO)_4\{\mu\text{-}\eta^2\text{:}\eta^3\text{-}HC{\equiv}C{-}CH_2\}]^+$. Clearly, a kind of level crossing between Mo1−Mo2 and Mo1−C5 antibonding orbitals occurs when going from $[Mo_2Cp_2(CO)_4\{\mu\text{-}\eta^2\text{:}\eta^3\text{-}HC{\equiv}C{-}CH_2\}]^+$ to $[Mo_2Cp_2(CO)_4\{\mu\text{-}\eta^2\text{:}\eta^3\text{-}HC{\equiv}C{-}CR_2\}]^+$. This crossing is avoided[25] and is actually dispersed over a set of several levels due to the large orbital intermixing allowed by the low symmetry of the complexes.

A better view of this avoided level crossing can be obtained by constructing a Walsh diagram associated with the variation of the Mo1−C5 distance. Figure 9 shows this Walsh diagram computed for the model $[Mo_2Cp_2(CO)_4\{\mu\text{-}\eta^2\text{:}\eta^3\text{-}HC{\equiv}C{-}CH_2\}]^+$, the geometry of which was derived from the experimental structure of $[Mo_2Cp_2(CO)_4\{\mu\text{-}\eta^2\text{:}\eta^3\text{-}HC{\equiv}C{-}C(H)(Me)\}]^+$ [15] (see Experimental Section). In this diagram, the Mo1−C5 distance varies from 2.13 to 3.45 Å. The avoided crossing between the two lowest vacant orbitals is evident. The LUMO goes down in energy significantly on the right side of Figure 9 as it increases its localization on C5. It can be correlated on the left side of Figure 9 to higher Mo1−C5 antibonding levels through several avoided crossings.

Although these EH results cannot be taken quantitatively, we think that they provide a nice rationalization of the experimental results. Compounds with short Mo1−C5 distances are situated on the left side of the avoided crossing. The addition of one electron in their LUMO is expected to somewhat lengthen the Mo1−Mo2 and the CO bonds but to only have a weak effect on the Mo1−C5 bond. These structural changes within the radical may be responsible for the large ΔE_p observed. A reorientation of the C3−C4−C5 ligand is also possible.[26] The experimental results (one-electron reduction) show that the structure change is not sufficient to reach the stage where the avoided crossing occurs. The SOMO/LUMO gap in the rearranged radical must be large enough to provide this species some stability since it is sufficiently long-lived to be detected by cv (R1 = H, R2 = Me or Et), even at slow scan rate when R1 = H, R2 = Et (v = 0.02 V/s, $(i_p^a/i_p^c) = 0.26$, CH_2Cl_2−Bu_4NPF_6). Furthermore, the absence of the oxidation peak of the radical in the cv (R1 = H, R2 = Me, slow scan rate) can be due to the occurrence of a second chemical step, the product-forming reaction (see below). This stabilization of the neutral radical does not overcome

(23) Cordier, C. Ph.D. Thesis, University Pierre et Marie Curie, Paris, France, 1991.

(24) Ruffolo, R.; Decken, A.; Girard, L.; Gupta, H. K.; Brook, M. A.; McGlinchey, M. J. *Organometallics* **1994**, *13*, 4328.

(25) Albright, T. A. *Tetrahedron* **1982**, *38*, 1339.

(26) For electron-transfer-induced reorientation of an alkyne ligand, see: Osella, D.; Gobetto, R.; Montangero, P.; Zanello, P.; Cinquantini, A. *Organometallics* **1986**, *5*, 1247. Rumin, R.; Robin-Le Guen, F.; Talarmin, J.; Pétillon, F. Y. *Organometallics* **1994**, *13*, 1155 and references therein. For alkyne ligands in an unusual coordination geometry, see: Ahmed, K. J.; Chisholm, M. H.; Folting, K.; Huffman, J. C. *Organometallics* **1986**, *5*, 2171. Calhorda, M. J.; Hoffmann, R. *Organometallics* **1986**, *5*, 2181. Cotton, F. A.; Feng, X. *Inorg. Chem.* **1990**, *29*, 3187.

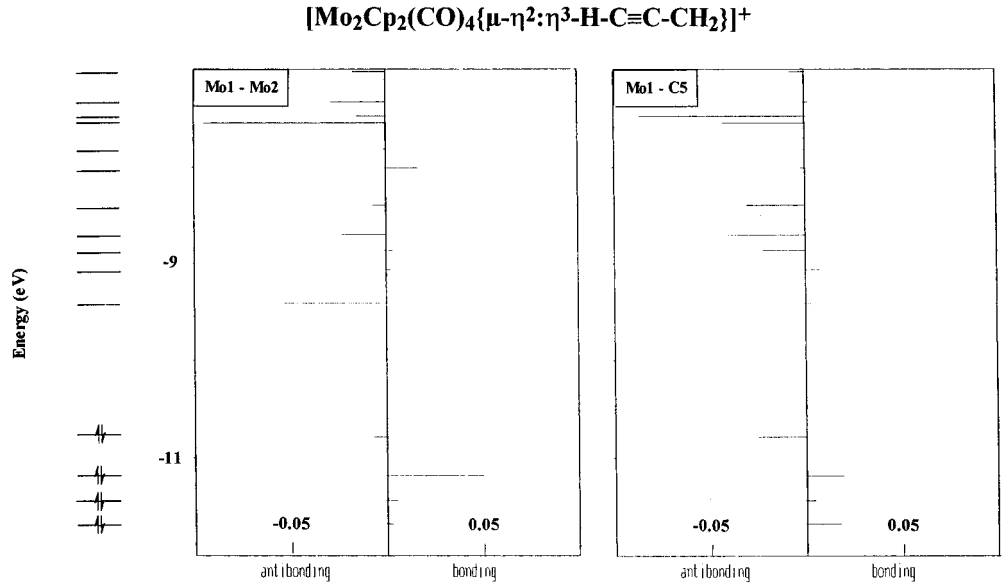

Figure 7. CACAO plots of the MO-level ordering and of the Mo1−Mo2 and Mo1−C5 orbital to orbital overlap populations of the model $[Mo_2Cp_2(CO)_4\{\mu\text{-}\eta^2\text{:}\eta^3\text{-}HC{\equiv}C{-}CH_2\}]^+$ (Mo1−C5 = 2.44 Å).

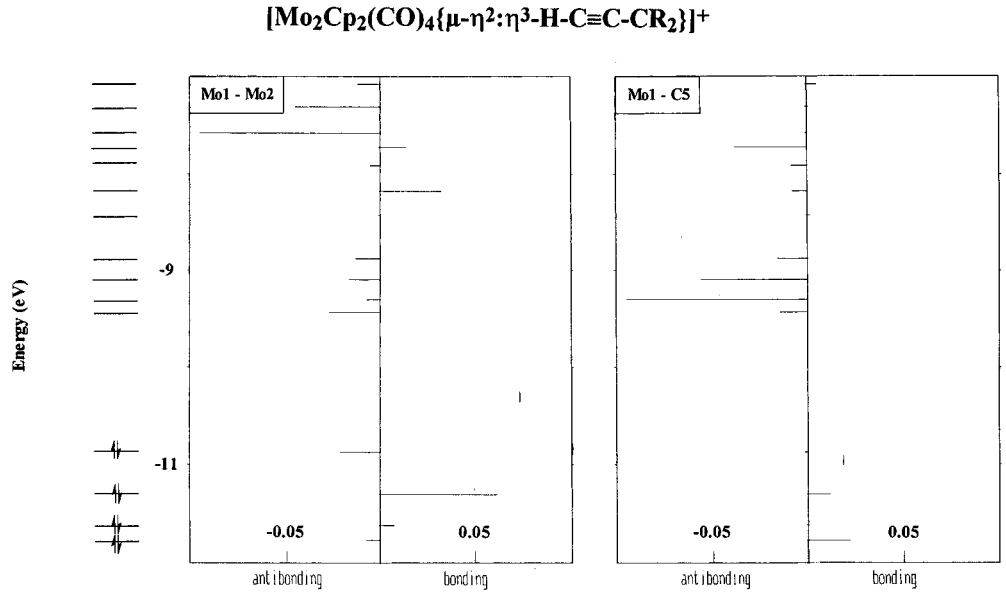

Figure 8. CACAO plots of the MO-level ordering and of the Mo1−Mo2 and Mo1−C5 orbital to orbital overlap populations of the model $[Mo_2Cp_2(CO)_4\{\mu\text{-}\eta^2\text{:}\eta^3\text{-}HC{\equiv}C{-}CR_2\}]^+$ (Mo1−C5 = 2.75 Å; R = H, see text).

the electrostatic repulsions and does not favor the addition of a second electron, which has to be transferred at a higher potential in order to force the avoided crossing.

Compounds with longer Mo1−C5 bonds are situated on the right side of (or at least very close to) the level crossing (Figure 9). The addition of one electron in their significantly Mo1−C5 antibonding LUMO should induce a concomitant lengthening of the Mo1−C5 separation. The resulting stabilization of the singly occupied HOMO of the neutral radical then makes possible the transfer of a second electron at the potential of the first addition ($|E°_1| \geq |E°_2|$). The stabilization of the HOMO of the resulting anion, which becomes largely C5 nonbonding, is such that an acceptable HOMO/LUMO gap is reached for this species to be thermodynamically stable (see the right side of Figure 9).

The Neutral Product-Forming Reaction. The electrochemical results indicate that the neutral product(s) of the controlled-potential reduction of the cationic complexes arises essentially from reactions of rearranged radical species. For the complexes with R1 = H, R2 = H, Me, or Et, the presence (or not) of the oxidation of this radical in the cv and the magnitude of the current for this oxidation process can be used as a qualitative estimate of the rates of the product-forming reactions. It is clear that the reaction rate decreases as the size of the substituents at C5 increases: when R1 = R2 = H the radical is not detected by cv ($v \leq 1$ V/s, Figure 1), whereas a very small oxidation peak is observed when R1 = H, R2 = Me (Figure 2, $v = 0.2$ V/s); when R1 = H, R2 = Et (Figure 3a) the radical is longer-lived but is yet quantitatively converted into the neutral products on the longer time scale of controlled-potential electrolyses (Figure 3c). In the case of the complexes with R1 = H, R2 = H, Me, the formation of the dimer on the cpe time scale demonstrates that a radical−radical coupling reaction follows the electron transfer

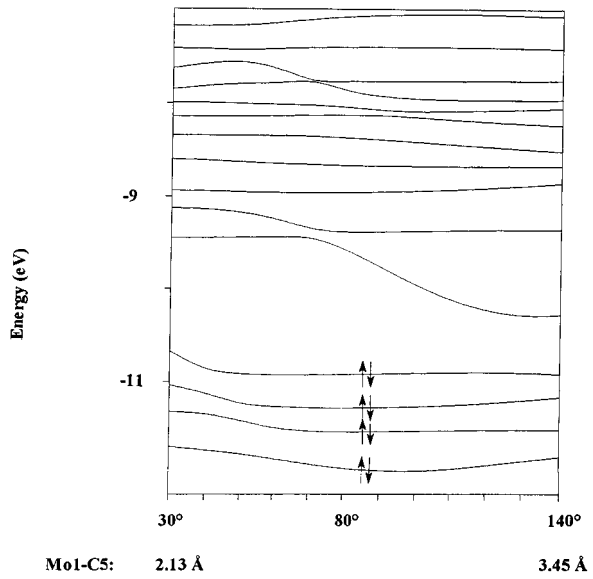

Figure 9. Walsh diagram of $[Mo_2Cp_2(CO)_4\{\mu\text{-}\eta^2\text{:}\eta^3\text{-}HC{\equiv}C{-}CH_2\}]^+$ associated with the variation of the Mo1−C5 distance (see Experimental Section for correspondence between the angle in the figure and the Mo1−C5 distance).

step (reaction I-2 of Scheme 1). The formation of the dimer on the cpe time scale from the radical detected on the cv time scale (R1 = H, R2 = Me) demonstrates that a coupling reaction occurred. The alternative that the dimer arises from reaction II-2 (Scheme 1) can be eliminated in the case of complex $\mathbf{2}^+$. Indeed, the fact that the reduction appears as a one-electron transfer on the cv time scale would require that reaction II-2 (Scheme 1) be fast. The current function for the reduction of $\mathbf{2}^+$ is independent of scan rate in the range from 0.2 to 1 V/s, while there is a substantial increase of i_p^a/i_p^c (i_p^a, peak current for the oxidation of the reduction product detected on the reverse scan; i_p^c, reduction peak current of $\mathbf{2}^+$) in the same range (i_p^a/i_p^c = 0.08 at 0.2 V/s; 0.19 at 0.5 V/s; 0.30 at 1 V/s). If the reduction product were $\mathbf{2}^-$, *i.e.*, $\mathbf{C}^-$ in Scheme 1, reaction II, one would expect an increase of the reduction current from a one-electron (no product detected on the reverse scan) toward a two-electron process (when the reduction product is observed). Therefore, one would expect that the plot of the current function *vs* scan rate deviates from linearity for scan rates increasing from 0.2 to 1 V/s. We did not observe such a deviation.

In the case of complex $\mathbf{1}^+$, the situation is less clear since no product other than the dimer is detected on the cv time scale for the scan rates used ($v \leq 1$ V/s). That the electrode process is a two-electron-transfer step followed by the fast chemical reaction II-2 cannot be completely ruled out. However, the general behavior of the carbenium complexes and the EHMO calculations makes this possibility unlikely.

In the case of the complexes with R1 = H, R2 = Et and R1 = R2 = Me (in CH_2Cl_2), the formation of the μ-alkyne and μ-enyne derivatives in similar amounts suggests that H-atom transfer involving two $[Mo_2Cp_2(CO)_4\{\mu\text{-}HC{\equiv}C{-}C(R1)(R2)\}]^\bullet$ radicals occurred.

The fact that the interaction of two $[Mo_2Cp_2(CO)_4\{\mu\text{-}HC{\equiv}C{-}C(R1)(R2)\}]^\bullet$ radicals lead to H-atom transfer for the complexes where R1 = H, R2 = Et and R1 = R2 = Me (in CH_2Cl_2), instead of the dimer formation observed for the less crowded complexes with R1 = H, R2 = H or Me, is not unexpected on steric grounds. It should be noted, however, that dimers have been obtained by chemical reduction of carbenium cations with bulky substituents such as R2 = Et[27] or Fc[2] (R1 = H).

The formation of neutral products from the reduction of the complexes with R1 = H, R2 = Fc and R1 = Me, R2 = Ph (and Me, in MeCN) on the cpe time scale also involves the $[Mo_2Cp_2(CO)_4\{\mu\text{-}HC{\equiv}C{-}C(R1)(R2)\}]^\bullet$ radical, thermodynamically unstable intermediate in a single-step two-electron-transfer process, Scheme 5.

We have shown that the final product(s) is (are) formed during the reduction of the parent cation *and* during the oxidation of the corresponding anion and that the stoichiometry of the electrolyses (number of electrons transferred *vs* yield of anion) is consistent only with the radical being the precursor of the final product(s). Although the neutral products of the cpe have not been isolated, the redox processes observed after controlled-potential reduction of the derivative with R1 = H, R2 = Fc indicate that $[Mo_2Cp_2(CO)_4\{\mu\text{-}HC{\equiv}C{-}CH_2\text{-}Fc)\}]$ has formed. The fact that no anion is produced from the reduction of $[Mo_2Cp_2(CO)_4\{\mu\text{-}\eta^2\text{:}\eta^3\text{-}HC{\equiv}C{-}C(Me)_2\}]^+$ when the electrolyses are performed in a CH_2Cl_2 electrolyte while some $[Mo_2Cp_2(CO)_4\{\mu\text{-}HC{\equiv}C{-}C(Me)_2\}]^-$ is formed in $MeCN{-}Bu_4NPF_6$ suggests that the source of the H atom is not the residual water of the solvent: it is indeed likely that MeCN, which was used as received, contains higher levels of residual water than CH_2Cl_2, which was distilled just before use. We believe that the H-atom source could be the solvent itself, the cation of the supporting electrolyte used in large excess being an alternative possibility. This is in contrast with the results obtained by Strelets *et al.* who reported a reaction of the *anions* with proton donors (residual water or cation of the supporting electrolyte).[3]

Conclusion

The main results of the electrochemical study of the $[Mo_2Cp_2(CO)_4\{\mu\text{-}\eta^2\text{:}\eta^3\text{-}HC{\equiv}C{-}C(R1)(R2)\}]^+$ complexes are summarized below. (1) The substituents R1 and R2 control the reduction process of the cations: we have shown that this is related to the Mo1−C5 distance observed in the solid. The complexes where these atoms are 2.4−2.6 Å apart undergo a one-electron reduction, whereas a larger separation (>2.7 Å) leads to a single-step two-electron-reduction process. (2) EHMO calculations provide a rationalization of the experimental results: these calculations show that for the complexes with the largest distance between Mo1 and C5 (2.75 Å), a small deformation of the geometry leads to a stabilization of the LUMO. This is the reason why the transfer of a second electron at the same potential as the first is possible. The small amplitude of the geometric change required to trigger the stabilization process, and thus the low reorganizational energy involved, account for the low energy barrier to electron transfer. In the case of the complexes with shorter Mo1···C5 distances, the transfer of a *single electron* must lead to a different reorganization of the complex, such as the lengthening of the metal−metal and C−O bonds. A modification of the geometry within the HC≡CC(R1)(R2) ligand or its reorientation with respect to the Mo−Mo bond are also

(27) Capon, J. F.; Cornen, S.; Le Berre-Cosquer, N.; Pichon, R.; Kergoat, R.; L'Haridon, P. *J. Organomet. Chem.* **1994**, *470*, 137.

Scheme 5

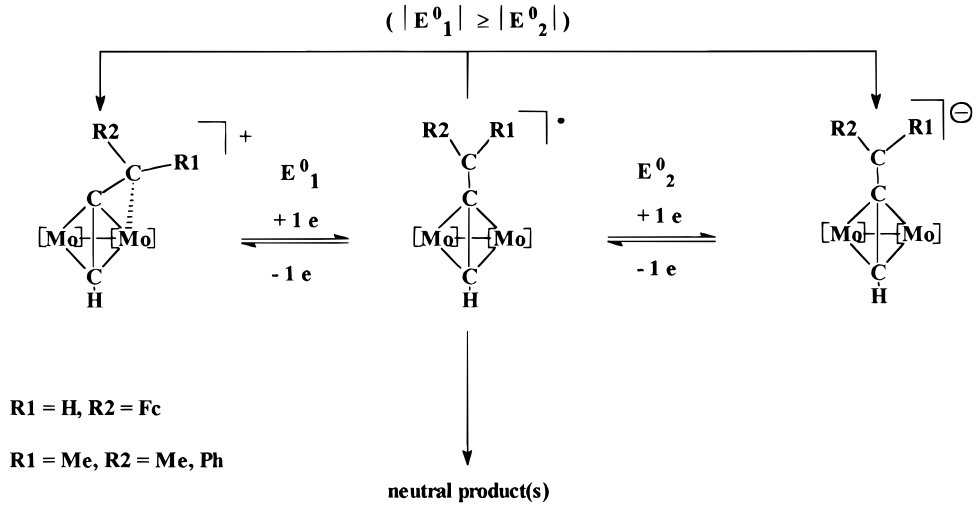

possible. (3) The neutral products obtained by electrolysis and detected on the cv time scale when R1 = H, R2 = H, Me, or Et arise from a reaction of a rearranged radical species. In the case of the complexes which undergo a two-electron reduction, the precursor of the final product(s) is also a radical, thermodynamically unstable intermediate in a single-step two-electron transfer. (4) A parallel can be made between the above results which show the effect of the R1 and R2 ligands on the reduction mechanism of the $[Mo_2Cp_2(CO)_4\{\mu\text{-}\eta^2\text{:}\eta^3\text{-}HC{\equiv}C{-}C(R1)(R2)\}]^+$ compounds and the studies of the fluxional processes in these complexes. It has been demonstrated that the energy barrier to isomerization decreases as the Mo1···C5 separation increases.[28] Therefore, it appears that the chemistry and the electrochemistry of the carbenium complexes are dominated by the R1 and R2 substituents, *via their steric effect on the Mo1−C5 separation*.

Experimental Section

Methods and Materials. All the experiments were carried out under an inert atmosphere, using Schlenk techniques for the syntheses. Tetrahydrofuran (thf) and CH_2Cl_2 were purified as described previously.[15] Acetonitrile (Carlo Erba or BDH, HPLC grade) was used as received. The preparation and purification of the supporting electrolyte $[Bu_4N][PF_6]$ are as described previously.[29] ^1H NMR spectra were recorded on a Bruker AC300 spectrometer. Shifts are relative to tetramethylsilane as an internal reference.

The $[Mo_2Cp_2(CO)_4\{\mu\text{-}\eta^2\text{:}\eta^3\text{-}HC{\equiv}C{-}C(R1)(R2)\}]^+$ complexes (R1 = R2 = H;[30] R1 = H, R2 = Me,[15] Et,[27] or Fc;[31] R1 = Me, R2 = Me[32] or Ph[33]) were prepared according to published procedures.

Electrochemistry. Cyclic voltammetry experiments and controlled-potential electrolyses were performed using Tacussel GCU or Tacussel PJT 120 potentiostats interfaced with a PAR model 175 waveform generator. The data were recorded on a SEFRAM TGM 164 X-Y recorder. For the coulometric experiments, Tacussel IG5N or IG6N electronic integrators were employed. The working electrode used for the cyclic voltammetry was a Metrohm 628 electrode with a vitreous carbon disk. The secondary electrode was either a carbon rod or a platinum wire. The reference electrode was a Ag/Ag^+ electrode. Ferrocene was added as an internal standard at the end of the experiments, and all of the potentials given throughout the paper are referred to the Fc/Fc^+ couple. The working electrode used for the controlled-potential electrolysis and coulometric experiments was a platinum foil or a Hg pool.

Preparative Controlled-Potential Electrolyses. The electrolyses intended to identify the reduction products of the $[Mo_2Cp_2(CO)_4\{\mu\text{-}\eta^2\text{:}\eta^3\text{-}HC{\equiv}C{-}C(R1)(R2)\}]^+$ complexes were carried out on the 100−200 mg scale (R1 = R2 = H, 0.1413 g, 0.252 mmol, thf-$[Bu_4N][PF_6]$; R1 = H, R2 = Me, 0.13 g, 0.22 mmol, CH_2Cl_2-$[Bu_4N][PF_6]$; R1 = H, R2 = Et, 0.18 g, 0.31 mmol, thf-$[Bu_4N][PF_6]$; R1 = R2 = Me, 0.1745 g, 0.3 mmol, CH_2Cl_2-$[Bu_4N][PF_6]$) at a potential 0.1 V more negative than the reduction potential of the complex at a Pt or a Hg pool electrode. After completion of the electrolysis (R1 = R2 = H, 0.93 F/mol, Hg pool cathode; R1 = H, R2 = Me, 0.80 F/mol, Pt cathode; R1 = H, R2 = Et, 0.89 F/mol, Hg pool cathode; R1 = R2 = Me, 0.96 F/mol, Pt cathode), the catholyte was canulated in a Schlenk flask under N_2 or Ar. The solvent was evaporated under vacuum, and the residue was extracted several times with pentane. The filtrates were taken to dryness, and the solid was dried under vacuum. ^1H NMR spectroscopy of the solid showed the formation of the dimer for R1 = R2 = H and R1 = R2 = Me (two stereoisomers), whereas a mixture of the μ-alkyne and μ-enyne complexes was obtained for R1 = H, R2 = Et (60:40) and R1 = R2 = Me (*ca.* 50:50).

EH Calculations. All of the calculations were carried out within the standard extended Hückel formalism[34] using the modified Wolfsberg−Helmoltz formula.[35] The CACAO5.0 package developped by Mealli and Proserpio was used.[36] Standard atomic parameters were taken for H, C, and O.[34] The exponents (ζ) and the valence shell ionization potential (H_{ii} in eV) used for Mo are the standard CACAO parameters,[36] *i.e.*, respectively, 1.956 and −8.34 for 5s, 1.921 and −5.24 for 5p. The H_{ii} value for 4d was −10.50. A linear combination of two Slater-type orbitals ($\zeta_1 = 4.54$, $c_1 = 0.5899$; $\zeta_2 = 1.900$, $c_2 = 0.5899$) was used to represent the atomic 4d orbitals. It

(28) Glalkhov, M. V.; Bakhmutov, V. I.; Barinov, I. V.; Reutov, O. A. *J. Organomet. Chem.* **1991**, *421*, 65.
(29) Gloaguen, F.; Le Floch, C.; Pétillon, F. Y.; Talarmin, J.; El Khalifa, M.; Saillard, J. Y. *Organometallics* **1991**, *10*, 2004.
(30) El Amouri, H.; Gruselle, M.; Besace, Y.; Vaissermann, J.; Jaouen, G. *Organometallics* **1994**, *13*, 2244.
(31) Capon, J. F.; Le Berre-Cosquer, N.; Leblanc, B.; Kergoat, R. *J. Organomet. Chem.* **1996**, *508*, 31.
(32) Froom, S. F. T.; Green, M.; Nagle, K. R.; Williams, D. J. *J. Chem. Soc., Chem. Commun.* **1987**, 1305.
(33) Capon, J. F.; Le Berre-Cosquer, N.; Bernier, S.; Pichon, R.; Kergoat, R.; L'Haridon, P. *J. Organomet. Chem.* **1995**, *487*, 201.
(34) Hoffmann, R. *J. Chem. Phys.* **1963**, *39*, 1397. Hoffmann, R.; Lipscomb, W. N. *J. Chem. Phys.* **1962**, *36*, 2179.
(35) Ammeter, J. H.; Bürgi, H. B.; Thibeault, J. C.; Hoffmann, R. *J. Am. Chem. Soc.* **1978**, *100*, 3686.
(36) Mealli, C.; Proserpio, D. M. *J. Chem. Educ.* **1990**, *67*, 399.

has been checked that a reasonable variation of the Mo parameters does not modify the qualitative conclusions of this study.

The molecular geometries considered in the calculations for the $[Mo_2Cp_2(CO)_4\{\mu\text{-}\eta^2\text{:}\eta^3\text{-}HC{\equiv}C{-}CH_2\}]^+$ and $[Mo_2Cp_2(CO)_4\{\mu\text{-}\eta^2\text{:}\eta^3\text{-}HC{\equiv}C{-}CR_2\}]^+$ models have been taken from the available published structural data of the $[Mo_2Cp_2(CO)_4\{\mu\text{-}HC{\equiv}C{-}CH_2\}]^+$ and $[Mo_2Cp_2(CO)_4\{\mu\text{-}HC{\equiv}C{-}CMe_2\}]^+$ complexes,[20] respectively. They have been completed with the experimental data of $[Mo_2Cp_2(CO)_4\{\mu\text{-}\eta^2\text{:}\eta^3\text{-}HC{\equiv}C{-}C(H)(Me)\}]^+$.[15] The model named $[Mo_2Cp_2(CO)_4\{\mu\text{-}\eta^2\text{:}\eta^3\text{-}HC{\equiv}C{-}CR_2\}]^+$ is a simplification of the compound with R = Me,[20] in which the Me groups have been changed into H atoms, keeping the same C−R bond orientation. The Walsh diagram of Figure 9 was calculated with a model of $[Mo_2Cp_2(CO)_4\{\mu\text{-}\eta^2\text{:}\eta^3\text{-}HC{\equiv}C{-}C(H)(Me)\}]^+$.[15] In this calculation, the Mo1−C5 distance was varied by rotating the C3−C4−C5 ligand about the C3−C4 vector (Scheme 4), everything else being constant. The corresponding dihedral angle varies from 30° (Mo1−C5 = 2.13 Å) to 140° (Mo1−C5 = 3.45 Å) (Figure 9). In all of the computed models, all of the C−H distances were set equal to 1.09 Å. It has been checked that small variations of the bond distances and angles within the $Mo_2Cp_2(CO)_4$ and HC≡C−C(R1)(R2) fragment do not significantly modify the computed results.

Acknowledgment. The CNRS (Centre National de la Recherche Scientifique) and the Université de Bretagne Occidentale are acknowledged for financial support to this work. The authors are grateful to Dr. M. Gruselle for translating the paper in ref 3 and for helpful discussions and comments. J.F.C. is grateful to MESR (Ministère de l'Enseignement Supérieur et de la Recherche) for providing a studentship.

OM970341U